Inorg. Chem. **2007**, *46*, 10907–10912

Thermodynamics of Oxygen Activation by Macrocyclic Complexes of Rhodium

Ewa Szajna-Fuller and Andreja Bakac*

Ames Laboratory, Iowa State University, Ames, Iowa 50011

Received August 1, 2007

The oxidation of $ABTS^{2-}$ [2,2′-azino-bis(3-ethylbenzothiazoline-6-sulfonate)] with a superoxorhodium(III) complex, $L^2(H_2O)RhOO^{2+}$ (L^2 = *meso*-hexamethylcyclam) is characterized by an acid-dependent equilibrium constant, $\log(K_e/[H^+]) = 4.91 \pm 0.10$ in the pH range of 4.89–6.49. This equilibrium constant was used to calculate the reduction potential for the $L^2(H_2O)RhOO^{2+}/L^2(H_2O)RhOOH^{2+}$ couple, $E^0 = 0.97$ V vs NHE. The pH dependence of the kinetics of the $L^2(H_2O)RhOOH^{2+}/I^-$ reaction yielded the acid dissociation constant for the coordinated water in $L^2(H_2O)RhOOH^{2+}$, $pK_a = 6.9$. Spectrophotometric pH titrations provided $pK_a = 6.6$ for the superoxo complex, $L^2(H_2O)RhOO^{2+}$. The combination of the two pK_a values with the reduction potential measured in acidic solutions yielded the reduction potential $E^0 = 0.95$ V for the $L^2(HO)RhOO^{+}/L^2(HO)RhOOH^{+}$ couple. Thermochemical calculations yielded the bond-dissociation free energy of the $L^2(H_2O)RhOO–H^{2+}$ bond as 315 kJ/mol at 298 K.

Introduction

Metal-based intermediates generated in the process of oxygen activation by transition-metal complexes are capable of oxidizing organic substrates by a variety of mechanisms, including electron transfer, hydrogen or oxygen atom transfer, and hydride transfer. Kinetic data for reactions with substrates are becoming increasingly available,[1−6] but thermodynamic information, with the exception of equilibrium constants for oxygen binding,[7−11] is much more limited.[3,12−17] The (typically) short lifetimes and low concentrations of such species require fast and sensitive methods that are not routinely available and will most likely have to be developed specifically for a particular intermediate or class of intermediates.

Here, we report some new thermodynamic data for macrocyclic superoxo and hydroperoxo rhodium(III) complexes, $L^2(H_2O)RhOO^{2+}$ and $L^2(H_2O)RhOOH^{2+}$ (L^2 = *meso*-hexamethylcyclam), both of which are reasonably stable in aqueous solutions in a wide range of pH. Our approach utilized a combination of kinetic and equilibrium measurements to determine reduction potentials, bond-dissociation free energies (BDFE), and acidity constants.

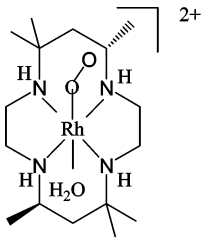

$L^2(H_2O)RhOO^{2+}$

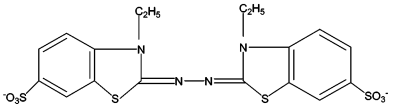

$ABTS^{2-}$

* To whom correspondence should be addressed. E-mail: bakac@ameslab.gov.

(1) Kovaleva, E. G.; Neibergall, M. B.; Chakrabarty, S.; Lipscomb, J. D. *Acc. Chem. Res.* **2007**, *40*, 475−483.
(2) Korendovych, I. V.; Kryatov, S. V.; Rybak-Akimova, E. V. *Acc. Chem. Res.* **2007**, *40*, 510−521.
(3) Bakac, A. *Prog. Inorg. Chem.* **1995**, *43*, 267−351.
(4) Bakac, A. *Adv. Inorg. Chem.* **2004**, *55*, 1−59.
(5) Bakac, A. *J. Am. Chem. Soc.* **2002**, *124*, 9136−9144.
(6) Shearer, J.; Zhang, C. X.; Zakharov, L. N.; Rheingold, A. L.; Karlin, K. D. *J. Am. Chem. Soc.* **2005**, *127*, 5469−5483.
(7) Simandi, L. I. *Catalytic Activation of Dioxygen by Metal Complexes*; Kluwer Academic Publishers: Dordrecht/Boston/London, 1992; Chapter 1.
(8) Bakac, A. *Coord. Chem. Rev.* **2006**, *250*, 2046−2058.
(9) Jones, R. D.; Summerville, D. A.; Basolo, F. *Chem. Rev.* **1979**, *79*, 139−179.
(10) Martell, A. E. *Acc. Chem. Res.* **1982**, *15*, 155−162.
(11) Falab, S.; Mitchell, P. R. *Adv. Inorg. Bioinorg. Mech.* **1984**, *3*, 311−377.
(12) Geiger, T.; Anson, F. C. *J. Am. Chem. Soc.* **1981**, *103*, 7489−7496.
(13) Kang, C.; Anson, F. C. *Inorg. Chem.* **1994**, *33*, 2624−2630.
(14) Kang, C.; Anson, F. C. *Inorg. Chem.* **1995**, *34*, 2771−2780.
(15) Roth, J. P.; Yoder, J. C.; Won, T. J.; Mayer, J. M. *Science* **2001**, *294*, 2524−2526.
(16) Gupta, R.; MacBeth, C. E.; Young, V. G., Jr.; Borovik, A. S. *J. Am. Chem. Soc.* **2002**, *124*, 1136−1137.
(17) Goldsmith, C. R.; Jonas, R. T.; Stack, T. D. P. *J. Am. Chem. Soc.* **2002**, *124*, 83−96.

10.1021/ic7015337 CCC: $37.00
Published on Web 11/07/2007

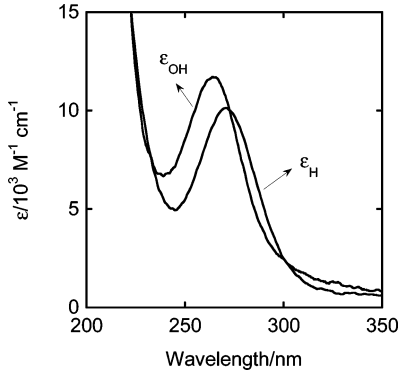

Figure 1. UV spectra of $L^2(H_2O)RhOO^{2+}$ (ϵ_H) and $L^2(HO)RhOO^+$ (ϵ_{OH}).

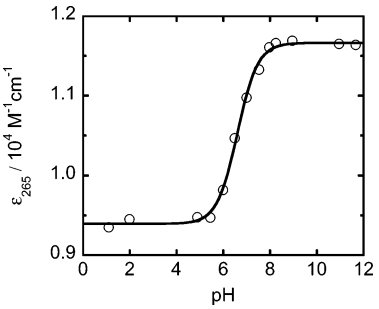

Figure 2. Plot of ϵ_{obs} against pH for $L^2(H_2O)RhOO^{2+}$. The line is a fit to eq 2.

Experimental Section

Solutions of $L^2(H_2O)RhOO^{2+}$ were prepared from the photochemically generated Rh(II) precursor and excess O_2.[18] The hydroperoxo complex, $L^2(H_2O)RhOOH^{2+}$, was prepared by the stoichiometric reduction of an air-free solution of the superoxo species with $Ru(NH_3)_6^{2+}$. In these experiments, the superoxo complex was degassed with a stream of argon for no longer than 10 min to minimize the losses caused by the slow dissociation of O_2 under anaerobic conditions. The tetraammine hydroperoxide, $(NH_3)_4(H_2O)RhOOH^{2+}$, was prepared from the hydride and molecular oxygen in alkaline solutions[19,20] followed by the addition of the buffer to attain the desired pH. Perchloric acid, lithium perchlorate, and sodium iodide (all Fisher), diammonium 2,2′-azinobis(3-ethylbenzothiazoline-6-sulfonate) ($(NH_4)_2$ABTS) and $Ru(NH_3)_6Cl_3$ (both Aldrich), and 2-(*N*-morpholino)ethanesulfonic acid (MES), piperazine-*N*,*N*′-bis(4-butanesulfonic acid) (PIPBS), and 2-(*N*-morpholino)-butanesulfonic acid (MOBS) (all GFS Chemicals) were used as received. The pH of reaction solutions was adjusted with $HClO_4$ (pH ≤3), NaOH (pH ≥11), and buffers (MES, PIPBS, and MOBS, pH 5.5−9) and measured with a Corning 320 pH meter after the completion of each experiment. The constant ionic strength of 0.10 M was maintained with lithium perchlorate. In-house distilled water was further purified by passage through a Barnstead EASYpure III system.

The equilibrium constant determination for the $L^2(H_2O)RhOO^{2+}/ABTS^{2-}$ reaction utilized limiting concentrations of $L^2(H_2O)RhOO^{2+}$ (0.015−0.058 mM) and a 2−100-fold excess of $ABTS^{2-}$. The absolute concentrations of $ABTS^{2-}$ depended on the pH and were chosen so that the reaction proceeded to 20−80% completion. The $L^2(H_2O)RhOOH^{2+}/I^-$ reaction was studied in the pH range of 3.00 ≤ pH ≤ 7.55. The concentration of the hydroperoxide was kept at 0.020 mM and that of iodide was kept at 14−94 mM.

(18) Bakac, A. *J. Am. Chem. Soc.* **1997**, *119*, 10726−10731.
(19) Pestovsky, O.; Bakac, A. *J. Am. Chem. Soc.* **2002**, *124*, 1698−1703.
(20) Vasbinder, M.; Bakac, A. *Inorg. Chem.* **2007**, *46*, 2921−2928.

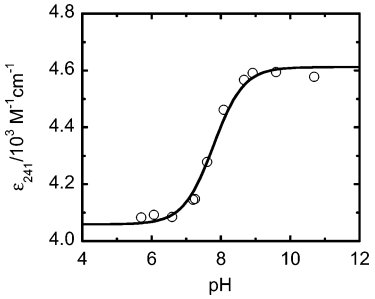

Figure 3. Plot of ϵ_{obs} against pH for $(NH_3)_4(H_2O)RhOOH^{2+}$. The line is a fit to eq 2.

Table 1. Spectral Data for the Complexes Used in This Work

complex	λ_{max} ($\epsilon/10^3$ M^{-1} cm^{-1})	λ_{titr} ($\epsilon/10^3$ M^{-1} cm^{-1})[a]	source
$L^2(H_2O)RhOO^{2+}$	272 (10.0)	265 (9.39)	ref 4
$L^2(HO)RhOO^+$	265 (11.6)	265 (11.7)	this work
$(NH_3)_4(H_2O)RhOOH^{2+}$	241 (4.0)	241 (4.06)	refs 4, 21
$(NH_3)_4(HO)RhOOH^+$	232 (5.2)	241 (4.61)	this work

[a] λ_{titr} = titration wavelength.

UV−vis spectral and kinetic measurements utilized a Shimadzu 3101 PC spectrophotometer at 25.0 ± 0.2 °C. Kinetic analyses were performed with *KaleidaGraph 3.6* PC software.

Results

Acidity Constants of $L^2(H_2O)RhOO^{2+}$ and $(NH_3)_4(H_2O)RhOOH^{2+}$. Acidity constants were determined from the effect of pH on the UV spectra. For $L^2(H_2O)RhOO^{2+}$ (eq 1), the spectra were collected in the pH range of 1.1 ≤ pH ≤ 11.9. The acidity constant was derived from the data obtained at 265 nm where the absorbance difference for the aqua and hydroxo forms was the largest (Figure 1). For each experiment, the absorbance was divided by the total concentration of the superoxo complex to obtain ϵ_{obs}, which is plotted against the pH in Figure 2. The data were fitted to eq 2, where ϵ_H (9.39×10^3 M^{-1} cm^{-1}) and ϵ_{OH} (1.17×10^4 M^{-1} cm^{-1}) represent the molar absorptivities of $L^2(H_2O)RhOO^{2+}$ and $L^2(OH)RhOO^+$, respectively, at 265 nm (Table 1). The fit yielded $K_a = (2.50 \pm 0.22) \times 10^{-7}$ M ($pK_a = 6.60$).

$$L^2(H_2O)RhOO^{2+} \rightleftarrows L^2(OH)RhOO^+ + H^+ \quad K_a \qquad (1)$$

$$\epsilon_{obs} = \frac{\epsilon_{OH}K_a + \epsilon_H[H^+]}{K_a + [H^+]} \qquad (2)$$

The pK_a value of $(NH_3)_4(H_2O)RhOOH^{2+}$ (eq 3) was determined by analogous treatment of the absorbance at 241 nm in the pH range of 5.7−10.7 and using the molar absorptivities in Table 1. The fit in Figure 3 yielded $K_a = (1.65 \pm 0.29) \times 10^{-8}$ M ($pK_a = 7.8$).

$$(NH_3)_4(H_2O)RhOOH^{2+} \rightleftarrows (NH_3)_4(OH)RhOO^+ + H^+ \quad K_a \qquad (3)$$

Reduction Potential for $(H_2O)L^2RhOO^{2+}/(H_2O)L^2RhOOH^{2+}$. The potential was derived from the equilibrium constant for the reduction of $(H_2O)L^2RhOO^{2+}$ with $ABTS^{2-}$ and the known reduction potential for the $ABTS^{\bullet-}/$

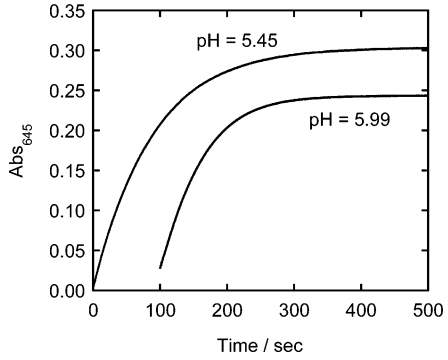

Figure 4. Growth in absorbance at 645 nm at two different acid concentrations for the reaction between 0.099 mM $ABTS^{2-}$ and $L^2(H_2O)RhOO^{2+}$ (0.0408 mM at pH 5.45 and 0.057 mM at pH 5.99). The lower curve was offset by 100 s for clarity.

Table 2. Equilibrium Data for the Reduction of $L^2(H_2O)RhOO^{2+}$ with $ABTS^{2-}$ [a]

$[H^+]$/pH	K_e	$\log(K_e/[H^+])$	E/V[b]	$k_f/M^{-1}\,s^{-1}$ [c]
1.29×10^{-5}/4.89	1.39	5.03	0.977	90
3.55×10^{-6}/5.45	0.326	4.96	0.973	64
1.02×10^{-6}/5.99	0.0671	4.92	0.970	54
3.24×10^{-7}/6.49	0.0213	4.82	0.964	30

[a] At 25 °C and 0.10 M ionic strength. [b] Calculated potential (vs NHE) for the $L^2(H_2O)RhOO^{2+}/L^2(H_2O)RhOOH^{2+}$ couple. [c] Forward rate constant for reaction 4, estimated from initial rates.

$ABTS^{2-}$ couple.[22] The amount of $ABTS^{\bullet-}$ generated from $ABTS^{2-}$ and limiting amounts of $L^2(H_2O)RhOO^{2+}$ (eq 4) was determined from the absorbance increase at 645 nm ($\epsilon = 1.35 \times 10^4\ M^{-1}\ cm^{-1}$)[22] in a number of experiments using a range of reactant concentrations at $4.89 \le pH \le 6.49$, as illustrated in Figure 4.

$$L^2(H_2O)RhOO^{2+} + ABTS^{2-} \overset{H^+}{\rightleftharpoons} L^2(H_2O)RhOOH^{2+} + ABTS^{\bullet-} \quad (4)$$

The yields of $ABTS^{\bullet-}$ were used to calculate the remaining three equilibrium concentrations, taking into account the 1:1 stoichiometry of eq 4. All the concentrations were inserted into eq 5 to obtain the conditional equilibrium constant K_e at each pH. The data shown in Table 2 are limited to the range of $4.89 \le pH \le 6.49$. At pH <4.89, the equilibrium was shifted too far to the right even with a minimal excess of $ABTS^{2-}$, which made the calculations of the equilibrium constant highly imprecise. At the other extreme, i.e., in neutral and alkaline solutions, the radical $ABTS^{\bullet-}$ is too unstable for precise measurements.

$$K_e = \frac{[ABTS^{\bullet-}][L^2(H_2O)RhOOH^{2+}]}{[ABTS^{2-}][L^2(H_2O)RhOO^{2+}]} \quad (5)$$

As shown in Table 2, the equilibrium constant obtained by dividing the conditional equilibrium constant by $[H^+]$ remained reasonably unchanged, $\log(K_e/[H^+]) = 4.91 \pm 0.10$ over the pH range of 4.89−6.49, although the values do seem to follow a mild trend. This is probably caused by the small but real difference in the acidity constants for the superoxo and hydroperoxo complexes, which changes the equilibrium proportions of the various hydrolytic forms and, consequently, of the overall energetics of electron transfer as the pH approaches the pK_a value. The effect on the calculated reduction potential is, however, minimal in the experimental pH range.

The difference between the reduction potentials $E_{Rh} - E_{ABTS}$ was obtained from the data in Table 2 and the equation $\log(K_e/[H^+]) = (E_{Rh} - E_{ABTS})/0.059$, where $E_{ABTS} = 0.68$ V.[22] The derived value for E_{Rh} (eq 6) is 0.97 ± 0.01 V.

$$L^2(H_2O)RhOO^{2+} + H^+ + e^- \rightleftarrows L^2(H_2O)RhOOH^{2+} \quad E_{Rh} \quad (6)$$

The traces in Figure 4 are kinetically quite complex, with both forward and reverse reactions contributing under non-pseudo-first-order conditions. Full kinetic analysis was not carried out, but the forward rate constant was estimated from the initial rates under the assumption that the contribution from the reverse reaction is minimal during the early stages of the reaction. The values of the forward rate constant so obtained at different H^+ concentrations are also listed in Table 2.

pK_a of $L^2(H_2O)RhOOH^{2+}$. Unlike $(NH_3)_4(H_2O)RhOOH^{2+}$ (see above), the macrocyclic hydroperoxide $L^2(H_2O)RhOOH^{2+}$ exhibits no pronounced maxima in the UV spectrum. In addition, the diaqua and hydroxoaqua species, $L^2(H_2O)_2Rh^{3+}$ and $L^2(H_2O)(OH)Rh^{2+}$, which are present at a 20−30% level as natural impurities in solutions of the hydroperoxo complex, also exhibit intense but featureless UV spectra and are also subject to acid/base equilibria. This combination would make questionable any determination of the acidity constant of $L^2(H_2O)RhOOH^{2+}$ from the effect of pH on the UV spectra of such mixtures.

We thus searched for a different, more reliable method that would be exclusively sensitive to the acid/base equilibria of the hydroperoxo species and unaffected by the presence of variable amounts of the aqua and/or aquahydroxo species. To this goal, we chose a kinetic approach and turned to the $L^2(H_2O)RhOOH^{2+}/I^-$ reaction (eqs 7−9), which we have studied earlier in strongly acidic solutions ($[H^+] \ge 0.010$ M).[23] Under such conditions, the reaction exhibits a first-order dependence on $[H^+]$ (eq 10), suggesting that a minor but highly reactive protonated form of the hydroperoxide, $L^2(H_2O)Rh(H_2O_2)^{3+}$, is the only reactive rhodium species.

$$L^2(H_2O)RhOOH^{2+} + I^- + H^+ \rightarrow L^2(H_2O)RhOH^{2+} + HOI \quad k_H \quad (7)$$

$$HOI + I^- + H^+ \rightleftarrows I_2 + H_2O \quad (8)$$

$$I_2 + I^- \rightleftarrows I_3^- \quad (9)$$

$$-d[L^2(H_2O)RhOOH^{2+}]/dt = k_H[L^2(H_2O)RhOOH^{2+}][I^-][H^+] \quad (10)$$

(21) Endicott, J. F.; Wong, C.-L.; Inoue, T.; Natarajan, P. *Inorg. Chem.* **1979**, *18*, 450−454.
(22) Scott, S. L.; Chen, W.-J.; Bakac, A.; Espenson, J. H. *J. Phys. Chem.* **1993**, *97*, 6710−6714.
(23) Lemma, K.; Bakac, A. *Inorg. Chem.* **2004**, *43*, 4505−4510.

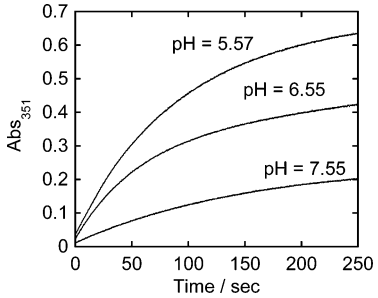

Figure 5. Absorbance increase at 351 nm in the reaction between $L^2(H_2O)RhOOH^{2+}$ (0.023 mM) and I^- (0.0944 M) as a function of pH.

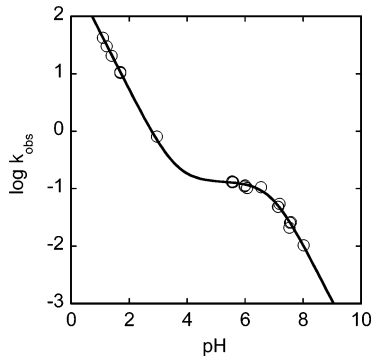

Figure 6. Plot of log *k* against pH for the oxidation of iodide ion with $L^2(H_2O)RhOOH^{2+}$. The line is a fit to eq 14.

At much lower $[H^+]$, where the concentration of $L^2(H_2O)Rh(H_2O_2)^{3+}$ is negligible, the reaction with $L^2(H_2O)RhOOH^{2+}$ should become measurable and much faster than that of the hydroxo form, $L^2(HO)RhOOH^+$. We confirmed these expectations in experiments at pH 3.00−7.55 and have used the data to determine the pK_a of coordinated water in $L^2(H_2O)RhOOH^{2+}$.

The growth in absorbance at 351 nm in solutions of different pH is illustrated in Figure 5. All three experiments utilized 0.0944 M I^- and 0.023 mM $L^2(H_2O)RhOOH^{2+}$. The yield of I_3^- was quantitative only at the lowest pH (5.57) and decreased systematically as the pH was raised. No O_2 was detected with an oxygen electrode in an experiment at pH 7.9 using 0.18 mM $L^2(H_2O)RhOOH^{2+}$ and 0.048 M I^- or in a control between 0.080 mM $L^2(H_2O)RhOOH^{2+}$ and either 0.060 or 0.11 mM I_2. Instead, significant amounts of $L^2(H_2O)RhOO^{2+}$ (about 40% of the initial concentration of $L^2(H_2O)RhOOH^{2+}$) were detected by the characteristic feature at 510 nm, $\epsilon = 430\ M^{-1}\ cm^{-1}$, and by increased absorbance around 265 nm.

To avoid complications (primarily caused by the change in stoichiometry) from the chemistry involving the product I_2/I_3^-, the kinetics data were obtained by the method of initial rates. These were determined from the build up of $[I_3^-]$ at 351 nm ($\epsilon = 2.6 \times 10^4\ M^{-1}\ cm^{-1}$) and divided by the product ($[L^2(H_2O)RhOOH^{2+}]_{tot} \times [I^-]$) to obtain the rate constant at a given $[H^+]$. Here, $[L^2(H_2O)RhOOH^{2+}]_{tot}$ represents the sum of the concentrations of both hydrolytic forms of the hydroperoxide, $[L^2(H_2O)RhOOH^{2+}] + [L^2(HO)RhOOH^+]$. This treatment yielded a consistent value of the rate constant at each pH, confirming first-order dependence on each reagent. The plot of the logarithm of the rate constant against pH is shown in Figure 6.

As shown earlier, the kinetics at high acidities exhibit linear dependence on $[H^+]$ (eq 10). Additional terms begin to contribute only at pH ≥3.5, so that the decrease in rate constant becomes less than linear. At an even higher pH, 4 ≤ pH ≤ 6.5, the rate constant levels off before the final decline at pH >6.5. The data at pH ≥3.5 constitute evidence for the existence of two species in acid−base equilibrium, the acidic form being much more reactive toward iodide (eqs 11−13).

$$L^2(H_2O)RhOOH^{2+} \rightleftarrows L^2(HO)RhOOH^+ + H^+ \quad K_a \qquad (11)$$

$$L^2(H_2O)RhOOH^{2+} + I^- \rightarrow \text{products} \quad k_{H_2O} \qquad (12)$$

$$L^2(HO)RhOOH^+ + I^- \rightarrow \text{products} \quad k_{OH} \qquad (13)$$

The rate law for the mechanism in eqs 7 and 11−13 is given in eq 14.

$$k_{obs} = \left(k_H[H^+] + \frac{k_{H_2O}[H^+] + k_{OH}K_a}{K_a + [H^+]}\right)[I^-] \qquad (14)$$

Figure 6 shows the fit to eq 14, which yielded the following parameters: $k_H = 525 \pm 16\ M^{-2}\ s^{-1}$, $k_{H_2O} = 0.132 \pm 0.005\ M^{-1}\ s^{-1}$, $k_{OH} = (5 \pm 16) \times 10^{-4}\ M^{-1}\ s^{-1}$, and $K_a = (1.20 \pm 0.14) \times 10^{-7}$ M. Clearly, the reactivity of $L^2(HO)RhOOH^{2+}$ is negligibly small in comparison with that of other forms. Setting $k_{OH} = 0$ has almost no effect on other parameters and only reduces the standard deviation for the K_a value, i.e., $k_H = 525 \pm 16\ M^{-2}\ s^{-1}$, $k_{H_2O} = 0.131 \pm 0.005\ M^{-1}\ s^{-1}$, and $K_a = (1.17 \pm 0.08) \times 10^{-7}$ M (pK_a = 6.9).

Discussion

The $L^2(H_2O)RhOO^{2+}/L^2(H_2O)RhOOH^{2+}$ reduction potential determined in this work is one of only a handful of such potentials for superoxo/hydroperoxo couples and, to the best of our knowledge, the first for a superoxorhodium complex. The value, 0.97 V, is quite close to the upper limit that we have estimated earlier for this couple on the basis of our inability to observe the reverse hydrogen atom transfer[20] in eq 15. Apparently, the true potential lay just outside the reach at the experimentally achievable concentrations and lifetimes of various species in eq 15.

$$(H_2O)_5CrOO^{2+} + L^2(H_2O)RhOOH^{2+} \rightleftarrows (H_2O)_5CrOOH^{2+} + L^2(H_2O)RhOO^{2+} \qquad (15)$$

The superoxorhodium potential is smaller, although not by a large amount, than those of similar dicationic superoxides of cobalt and chromium in Table 3, all of which are significantly weaker oxidants than $HO_2^\bullet$ ($E = 1.44$ V).[24] BDFE, calculated from the reduction potentials for the $H^+_{aq}/H^\bullet_{aq}$ (−2.30 V)[25] and $L(H_2O)MOO^{2+}/L(H_2O)MOOH^{2+}$ couples

(24) Bard, A. J.; Parsons, R.; Jordan, J. *Standard Potentials in Aqueous Solution*; Marcel Dekker: New York and Basel, 1985.
(25) Buxton, G. V.; Greenstock, C. L.; Helman, W. P.; Ross, A. B. *J. Phys. Chem. Ref. Data* **1988**, *17*, 513−886.

Table 3. Summary of Thermodynamic Data for Superoxo and Hydroperoxo Complexes

$L(H_2O)M$	E/V[a]	BDFE[b]	$pK_{a,MOO}$[c]	$pK_{a,MOOH}$[d]	source
$L^1(H_2O)Co^{2+}$	1.01[e]	318		8 ± 1	refs 12,26
$L^2(H_2O)Co^{2+}$	1.05[f]	322	6.42		refs 14,27
$(H_2O)_5Cr^{2+}$	1.03[g]	320			ref 13
$L^2(H_2O)Rh^{2+}$	0.97[h]	315	6.6	6.9−7.4	this work
$L^1(H_2O)Cr^{2+}$			4.9	5.6	ref 28
$L^2(H_2O)Cr^{2+}$				5.9	ref 29
H[i]	1.44	360	4.8[j]	11.7[k]	ref 24

[a] Reduction potential in V vs NHE for $L(H_2O)MOO^{2+}/L(H_2O)MOOH^{2+}$ couples at 1.0 M H^+. [b] Bond-dissociation free energies in kJ/mol at 298 K for MOO−H bonds. [c] pK_a of coordinated H_2O in superoxo complexes. [d] pK_a of coordinated H_2O in hydroperoxo complexes. [e] In 0.5 M $HClO_4$. [f] Estimated from $E = 0.99$ V at pH 1. [g] Estimated from $E = 0.97$ V at pH 1. [h] Determined in experiments at pH 5.0−6.5 at 0.10 M ionic strength; see text. [i] The couple is $HO_2^{\bullet}/H_2O_2$. [j] pK_a of $HO_2^{\bullet}$. [k] pK_a of H_2O_2.

(eqs 16−18) are also shown in Table 3. Obviously, hydrogen atom abstraction from metal hydroperoxides is thermodynamically much more favorable than that from H_2O_2. This difference is clearly reflected in the kinetics, as we have shown in our earlier work.[20]

$$L(H_2O)MOO^{2+} + H^+ + e^- \rightleftarrows L(H_2O)MOOH^{2+} \quad \Delta G_{MOO} \quad (16)$$

$$H^{\bullet}_{aq} \rightleftarrows H^+_{aq} + e^- \qquad \Delta G_H \qquad (17)$$

$$\text{Net:} \quad L(H_2O)MOO^{2+} + H^{\bullet}_{aq} \rightleftarrows L(H_2O)MOOH^{2+} \quad \text{BDFE} \quad (18)$$

The reaction between $L^2(H_2O)RhOOH^{2+}$ and I^- at pH >6 turned out to be more complex than that in acidic solutions. In our earlier work at pH ≤2, the chemistry in eq 19 and the stoichiometry $[L^2(H_2O)RhOOH^{2+}]_0/[I_2]_\infty = 1{:}1$ were firmly established.[23]

$$L^2(H_2O)RhOOH^{2+} + I^- \xrightarrow{I^-,H^+} L^2(H_2O)RhOH^{2+} + I_2/I_3^- + H_2O \quad (19)$$

These results were confirmed in the present work at pH 3 and 5.5, but the yields of I_3^- decreased as the pH increased above 6. Molecular O_2 was not observed; instead, large amounts of $L^2(H_2O)RhOO^{2+}$ were produced. These results rule out the chemistry analogous to that observed earlier in the $(NH_3)_4(H_2O)RhOOH^{2+}/Br^-$ reaction. In that case, O_2 was produced at the expense of Br_2 under conditions of low $[Br^-]$ and low $[H^+]$ (Scheme 1).[23]

The present data suggest that iodine/triiodide oxidizes $L^2(H_2O)RhOOH^{2+}$ to the superoxo complex. Experiments using freshly prepared $L^2(H_2O)RhOOH^{2+}$ and an excess of externally added I_2 in the absence of I^- have confirmed this hypothesis (see Results). Our experimental data were insufficient to establish the mechanism for this reaction, which falls beyond the scope of this work, but some possibilities can be ruled out. Almost certainly, the reaction does not proceed by single electron transfer, because the thermodynamics, as measured by one-electron reduction potentials for $L^2(H_2O)RhOO^{2+}/L^2(H_2O)RhOOH^{2+}$ (0.56 V at pH 7) and

Scheme 1

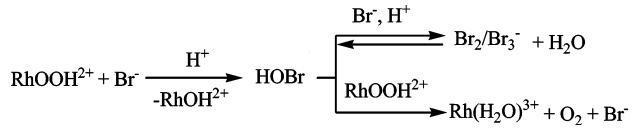

I_2/I_2^- (0.21 V)[30] are significantly uphill. A two-electron reaction, similar to that observed with Br_2 in Scheme 1, would seem somewhat more favorable at higher pH on the basis of the equilibrium hydrolysis constant for I_2 (eq 20)[31] and the two-electron reduction potential of HOI (0.57 V at pH 7).[24]

$$I_2 + H_2O \rightleftarrows HOI + I^- + H^+ \quad K = 5.3 \times 10^{-13}\ M^2 \qquad (20)$$

A two-electron reaction would, however, require that the initial rhodium product be quickly reduced by one electron before O_2 can dissociate. Either iodide or hydroperoxorhodium could act as reductants, but it is remarkable that a doubly oxidized hydroperoxo complex, most easily pictured as $L^2(H_2O)RhOO^{3+}$, should survive long enough to engage in a bimolecular reaction of any kind. Further work is needed before we can address this chemistry in more detail.

In the determination of the rate constant for the $L^2(H_2O)RhOOH^{2+}/I^-$ reaction in Figure 6, we used initial rates. Those, we believe, are unaffected by the $L^2(H_2O)RhOOH^{2+}/I_2$ side reaction, which should set in as the concentration of the generated I_2 builds up. Furthermore, in our calculations, we used only data from those experiments that gave ≥50% total yield of I_2/I_3^-. In the most unfavorable and unlikely case, i.e., if the $L^2(H_2O)RhOOH^{2+}/I_2$ reaction is fast even during the initial stages of the reaction when I_2 concentrations are very low (1−2 μM) and when 99% of that amount is present as the (presumably) unreactive I_3^- at our typical iodide concentration of ∼ 0.1 M, then the rate constants at pH >6 in Figure 6 could be up to a factor of 1.5 too small, and the true K_a value for $L^2(H_2O)RhOOH^{2+}$ could be as low as 4×10^{-8} M (pK_a 7.4). This is an unlikely possibility, but we cannot rule it out completely.

Having determined the potential for the $L^2(H_2O)RhOO^{2+}/L^2(H_2O)RhOOH^{2+}$ couple and the acidity constants for the superoxo and hydroperoxo complexes, we were able to calculate the potential for the $L^2(HO)RhOO^+/L^2(HO)RhOOH^+$ couple by combining eqs 1, 6, and 11, as shown in Scheme 2 below. This potential, 0.95 V (or 0.92 V if the pK_a value for $L^2(H_2O)RhOOH^{2+}$ is 7.4), shows that the superoxo complex is only mildly less oxidizing in alkaline solutions than it is in the presence of acid ($E = 0.97$ V) owing to the similarity in the acidity constants of coordinated waters in the superoxo and hydroperoxo complexes, 6.6 and 6.9 (or 7.4), respectively. This is consistent with the chemical similarity of the two complexes, an overall 2+ charge for

(26) Kumar, K.; Endicott, J. F. *Inorg. Chem.* **1984**, *23*, 2447−2452.
(27) Marchaj, A.; Bakac, A.; Espenson, J. H. *Inorg. Chem.* **1992**, *31*, 4164−4168.
(28) Pestovsky, O.; Bakac, A. *Dalton Trans.* **2005**, 556−560.
(29) Lemma, K.; Ellern, A.; Bakac, A. *Dalton Trans.* **2006**, 58−63.
(30) Stanbury, D. M. *Adv. Inorg. Chem.* **1989**, *33*, 69−138.
(31) Schmitz, G. *Int. J. Chem. Kinet.* **2004**, *36*, 480−493.

Scheme 2

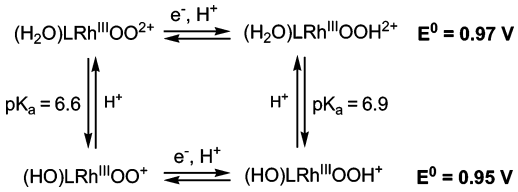

both, and the fact that positions trans to both the superoxo and hydroperoxo groups are kinetically labile.

The case of L^2Rh complexes in this work appears to be the first one where the thermodynamics of each individual step in the superoxo/hydroperoxo scheme for both aqua and hydroxo complexes have been determined. Only fractional data are available for a handful of other macrocyclic metal complexes, as shown in Table 3.

Throughout our discussion, we have assigned the pK_a value for $L^2(H_2O)RhOOH^{2+}$ to be that of coordinated water, although technically we cannot rule out the hydroperoxo group as the source of the observed acid/base chemistry. We prefer the former interpretation because a coordinated water should be more acidic than a coordinated hydroperoxide anion. Also, the measured pK_a value and the observed spectral changes are quite similar to those for the superoxo complex, which has H_2O as the only acidic site. Deprotonation of the hydroperoxo group has been observed for a number of hydroperoxo complexes, although not in aqueous solutions. Oftentimes, the loss of the proton is accompanied by the change in the binding mode from an end-on hydroperoxide to a side-on peroxide.[32−35]

(32) Takahashi, Y.; Hashimoto, M.; Hikichi, S.; Akita, M.; Moro-oka, Y. *Angew. Chem., Int. Ed.* **1999**, *38*, 3074−3077.
(33) Jensen, K. B.; McKenzie, C. J.; Nielsen, L. P.; Pedersen, J. Z.; Svendsen, H. M. *Chem. Commun.* **1999**, 1313−1314.
(34) Simaan, A. J.; Banse, F.; Mialane, P.; Boussac, A.; Un, S.; Kargar-Grisel, T.; Bouchoux, G.; Girerd, J. J. *Eur. J. Chem.* **1999**, 993−996.
(35) Ho, R. Y. N.; Roelfes, G.; Hermant, R.; Hage, R.; Feringa, B. L.; Que, L., Jr. *Chem. Commun.* **1999**, 2161−2162.

Conclusions

A combination of kinetic and equilibrium studies with reagents of known redox potentials and reactivity patterns has provided a convenient and *specific* method for the determination of several thermodynamic parameters for the superoxo/hydroperoxo rhodium complexes $L^2(H_2O)RhOO^{2+}$ and $L^2(H_2O)RhOOH^{2+}$. The kinetic approach to pK_a determinations has an obvious advantage over the standard titration methods in that it is selective and provides data only for the species of interest while ignoring other reagents in the same solution. The simultaneous presence of several different species with ionizable hydrogens is a common situation in studies of reactive intermediates, such as those generated in the process of oxygen activation, so that the development of additional species-specific methods will almost certainly be required in the future. From the reduction potential for the $L^2(H_2O)RhOO^{2+}/L^2(H_2O)RhOOH^{2+}$ couple (0.97 V vs NHE) and the acidity constants of the coordinated molecules of water in both complexes, the potential for the $L^2(HO)RhOO^{+}/L^2(HO)RhOOH^{+}$ couple was also obtained, $E = 0.95$ V. The two potentials are comparable owing to the similar acid dissociation constants of coordinated molecules of water in superoxo and hydroperoxo ions, pK_a = 6.60 and 6.9, respectively.

Acknowledgment. This manuscript has been authored under Contract No. DE-AC02-07CH11358 with the U.S. Department of Energy. The United States Government retains and the publisher, by accepting the article for publication, acknowledges that the United States Government retains a non-exclusive, paid-up, irrevocable, worldwide license to publish or reproduce the published form of this manuscript, or allow others to do so, for United States Government purposes.

IC7015337